



ISSN: 2617-6548

URL: [www.ijirss.com](http://www.ijirss.com)



## Performance evaluation of OMP, SVD, deep unfolding, and genetic algorithm-based hybrid beamforming for IRS-assisted mmwave MU-OFDM-mMIMO in B5G networks

Rita Abdal-Aziz<sup>1\*</sup>, Ali A. S. AlAbdullah<sup>2</sup>, Mahmod A. Alzubaidy<sup>3</sup>

<sup>1,2,3</sup>*Department of Communication Engineering, Ninevah University, Mosul, Iraq.*

Corresponding author: Rita Abdal-Aziz (Email: [rita.abdalaziz.eng22@stu.uoninevah.edu.iq](mailto:rita.abdalaziz.eng22@stu.uoninevah.edu.iq))

### Abstract

This paper examines the performance analysis of the hybrid beamforming algorithms, which are Orthogonal Matching Pursuit (OMP), Singular Value Decomposition (SVD), Deep Unfolding, and Genetic Algorithms (GA), in IRS-assisted MU-OFDM massive mMIMO systems operating in mmWave channels for B5G networks. This paper evaluates these algorithms across a comprehensive set of performance metrics, including Spectral Efficiency (SE), Energy Efficiency (EE), Bit Error Rate (BER), and Outage Probability, with an IRS configuration with 2-bit quantized phase shifts meticulously optimized to maximize the system sum rate. The research uses an advanced simulation framework to examine the algorithms' performance under different Signal-to-Noise Ratio (SNR) values, ranging from -10 dB to 30 dB, that reflect typical mmWave channel environments. The simulation results show that OMP performs better in achieving high SE and minimizing BER, especially at high SNR values, and GA is better at optimizing EE, which makes it suitable for energy-constrained scenarios. The inclusion of IRS technology significantly enhances the overall system reliability and efficiency, with a notable reduction in outage probability, which validates its potential as a key component in B5G network design. These results provide valuable insights into the practical implementation and optimization of hybrid beamforming strategies, which will guide the development of robust and efficient next-generation wireless communication systems.

**Keywords:** Beyond 5G, Bit error rate, Energy efficiency, Hybrid beamforming, IRS, mmWave, MU-OFDM-mMIMO, Outage Probability, Spectral Efficiency.

**DOI:** 10.53894/ijirss.v8i11.10820

**Funding:** This study received no specific financial support.

**History: Received:** 12 September 2025 / **Revised:** 7 October 2025 / **Accepted:** 10 October 2025 / **Published:** 5 November 2025

**Copyright:** © 2025 by the authors. This article is an open access article distributed under the terms and conditions of the Creative Commons Attribution (CC BY) license (<https://creativecommons.org/licenses/by/4.0/>).

**Competing Interests:** The authors declare that they have no competing interests.

**Authors' Contributions:** All authors contributed equally to the conception and design of the study. All authors have read and agreed to the published version of the manuscript.

**Transparency:** The authors confirm that the manuscript is an honest, accurate, and transparent account of the study; that no vital features of the study have been omitted; and that any discrepancies from the study as planned have been explained. This study followed all ethical practices during writing.

**Publisher:** Innovative Research Publishing

## 1. Introduction

Beyond 5G (B5G) networks are moving forward due to the growing need for high-speed data, energy efficiency, and reliable connectivity to support new use cases like holographic communication and massive IoT deployments [1]. Millimeter-wave (mmWave) communication operating in the 30 GHz to 300 GHz range has extensive bandwidth but suffers from substantial path loss and blockage issues [2]. The implementation of massive Multiple-Input Multiple-Output (mMIMO) and Multi-User Orthogonal Frequency Division Multiplexing (MU-OFDM) solves these problems through spatial multiplexing and frequency diversity, but the hardware complexity and power consumption persist as challenges. Hybrid beamforming, which combines analog and digital processing, provides a trade-off by minimizing the number of radio frequency (RF) chains [3].

The deployment of passive reflecting elements in Intelligent Reflecting Surface (IRS) technology creates a new paradigm by controlling phase shifts to improve signal propagation and enhance coverage and capacity in mmWave systems [4]. The paper investigates the performance of four hybrid beamforming methods: Orthogonal Matching Pursuit (OMP), Singular Value Decomposition (SVD), Deep Unfolding, and Genetic Algorithms (GA), in IRS-assisted MU-OFDM-mMIMO systems. This paper considers an IRS setup with 2-bit quantized phase shifts that are optimized to maximize the sum rate while assessing the system through Spectral Efficiency (SE), Energy Efficiency (EE), Bit Error Rate (BER), and Outage Probability. The thorough examination along with simulation findings establish a strong basis for future B5G network development.

Figure 1 illustrates a standard urban deployment scenario which uses an Intelligent Reflecting Surface (IRS) to overcome blockages between base stations and user equipment. The situation shows how IRS enables non-line-of-sight (NLoS) communications through buildings and other obstacles in crowded areas like cities:

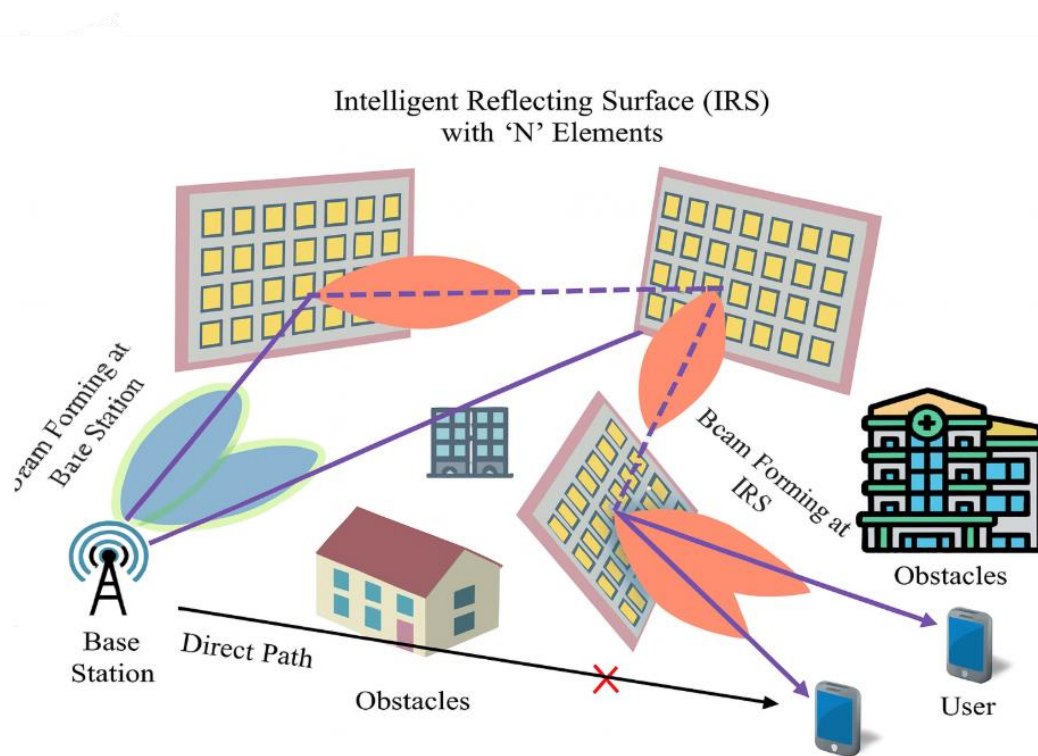


**Figure 1.**

Illustration of an IRS-assisted communication scenario in an urban environment, showing a blocked direct path and an IRS-reflected path

## 2. Literature Survey

Numerous studies have addressed hybrid beamforming strategies for IRS-assisted mmWave communication systems, spanning traditional optimization algorithms and modern deep learning-based approaches. This section presents a structured survey of recent literature, categorized according to algorithmic foundations such as compressed sensing, genetic algorithms, and deep unfolding techniques. By examining the capabilities, limitations, and performance outcomes of each method, we aim to highlight the evolution of beamforming design and identify research gaps addressed by our proposed framework.

Wang, et al. [5] propose a joint active and passive precoding strategy for IRS-aided mmWave systems. They formulate an optimization problem for hybrid beamforming, considering the phase shift control of IRS. Simulations reveal significant gains in spectral efficiency and energy efficiency. Their model assumes perfect channel state information and focuses on system-level performance. This work forms a baseline for IRS and hybrid beamforming co-design under ideal conditions.

Shi, et al. [6] introduce a deep-unfolding network for hybrid beamforming with symbol error minimization. The method unfolds iterative optimization into neural network layers for fast, interpretable inference. Results show competitive

performance with reduced computational complexity. Their model performs well under noisy conditions and varying channel environments. It offers a balance between deep learning flexibility and model-based reliability.

Koc, et al. [7] present a genetic algorithm (GA)-based approach for resource allocation in mmWave MU-MIMO-OFDM. The algorithm jointly optimizes beamforming weights and subcarrier allocation. It achieves better throughput and energy efficiency than conventional heuristics. The method is suitable for systems with constrained power and high user density. Their results support GA as a viable tool in practical large-scale systems.

Kang, et al. [8] propose a mixed-timescale deep-unfolding technique for joint channel estimation and beamforming. They separate fast and slow timescale components to adaptively train the model. Their approach outperforms traditional CSI-based schemes in non-stationary scenarios. It provides strong convergence and robustness for fast-varying channels. The study supports deep unfolding as a hybrid solution between data and model-driven designs.

Ikeagu, et al. [9] develop a lightweight deep learning model for hybrid beamforming in IRS-aided systems. Their framework is optimized for real-time inference on edge devices with limited computation. Simulation results demonstrate near-optimal performance with reduced complexity. This approach enables practical deployment of IRS-assisted hybrid MIMO. They target energy-efficient solutions for future wireless networks with hardware constraints.

Lee and Hong [10] present a low-complexity hybrid beamforming algorithm that uses only cascaded channel knowledge. They demonstrate that asymptotically optimal performance can be achieved without full CSI. Their approach simplifies system design in large-scale IRS-assisted MIMO. It is highly efficient and suitable for practical deployment in mmWave systems. The study highlights the benefits of bypassing full channel estimation for scalable designs.

Peng and Yang [11] address hybrid beamforming under imperfect CSI for mmWave massive MIMO. Their robust design algorithm maintains high spectral efficiency despite channel uncertainties. They use stochastic optimization techniques to mitigate estimation errors. Results show resilience against practical impairments in CSI acquisition. The work ensures reliable performance in dynamic and uncertain wireless environments.

Chen, et al. [12] propose a deep unfolded network for broadband IRS-aided mmWave OFDM systems. They focus on designing frequency-selective analog beamformers to address multipath channels. The system achieves high spectral efficiency across subcarriers. Their unfolded structure retains interpretability and computational efficiency. It bridges wideband signal processing with learning-based hybrid beamforming.

Srinivas and Borugadda [13] develop a DL-based channel estimation and adaptive hybrid beamforming framework. Their approach supports group-of-subarray architectures in mmWave massive MIMO. It enhances link reliability and spectral efficiency under hardware limitations. They use supervised learning to dynamically adapt beamformers. The system shows promising results in diverse channel and subarray configurations.

Yildirim, et al. [14] design hybrid beamforming techniques for terahertz MIMO systems using multiple RIS. They address joint optimization of multiple reflective surfaces with analog-digital precoding. Results demonstrate capacity gains in high-frequency THz environments. Their method enables scalable beamforming for ultra-dense deployments. The work supports THz-band communication as a future B5G/6G technology enabler.

Deka, et al. [15] present a comprehensive review of deep unfolding techniques in wireless systems. They classify models based on optimization strategy, network type, and application area. The review includes use cases in channel estimation, beamforming, and resource allocation. They highlight trade-offs in interpretability, complexity, and adaptability. This survey serves as a guide for applying unfolding in next-gen wireless protocols.

Rahkheir and Akhlaghi [16] propose joint hybrid precoding and multi-IRS optimization for MU-MISO systems. They co-design the passive IRS and active precoders using alternating optimization. Their simulations show significant throughput improvements over decoupled methods. The work supports multi-IRS architectures in complex environments. It demonstrates the advantage of integrating beamforming and IRS control holistically.

Luo, et al. [17] apply deep unfolding to hybrid relaying systems in mmWave networks. They focus on improving SNR and BER performance in amplify-and-forward relays. Their approach adapts the beamforming vectors through a learned unfolding framework. It achieves lower error rates and improved link reliability. This supports efficient relay operation in hybrid mmWave architectures.

Yang, et al. [18] propose a deep unfolding method for near-field channel estimation in 6G networks. They address spherical wavefront modeling in ultra-massive MIMO scenarios. The method enhances angle-delay resolution and estimation accuracy. Their network is tailored for near-field propagation under high-frequency bands. This contributes to more accurate beamforming in future dense deployments.

Saeed, et al. [19] design a lightweight DL model for channel estimation in large-scale RIS MIMO. The solution targets edge devices with constrained memory and computer capacity. Despite the lightweight design, it achieves near-optimal estimation accuracy. The system is tailored for energy-efficient 6G and IoT scenarios. Their work proves the viability of deploying DL at the wireless edge.

This survey presents a comprehensive exploration of recent advancements in hybrid beamforming strategies for IRS-assisted mmWave MU-OFDM-mMIMO systems. Traditional model-based approaches, such as joint precoding under perfect CSI and genetic algorithm optimization, provide solid performance foundations but often demand ideal conditions or significant computational resources. Emerging techniques, particularly those based on deep unfolding and lightweight deep learning, have demonstrated superior adaptability, scalability, and robustness in the face of practical constraints like imperfect CSI, near-field propagation, and hardware limitations. Moreover, innovations targeting THz frequencies and edge deployment highlight the expanding relevance of these methods in future 6G architectures. Collectively, these works confirm that hybrid approaches combining physical modeling and machine learning offer a promising pathway to meet the

stringent demands of B5G and beyond. Future research should further explore unified frameworks for joint IRS and hybrid beamforming design under realistic channel dynamics and system constraints.

### 3. System Model and Methodology

#### 3.1. System Model

The system under consideration is an IRS-assisted MU-OFDM-mMIMO setup operating at 28 GHz in the mmWave band. The base station (BS) is equipped with  $N_t = 64$  transmit antennas and  $N_{RF} = 8$  RF chains, serving  $K = 4$  users, each with  $N_r = 16$  receive antennas. The IRS consists of  $M = 100$  passive reflecting elements that adjust phase shifts to optimize signal propagation [4]. The mmWave channel for the  $k$ -th user,  $\mathbf{H}_k \in \mathbb{C}^{N_r \times N_t}$ , is modeled using the Saleh-Valenzuela framework [2].

$$\mathbf{H}_k = \sqrt{\frac{N_t N_r}{L}} \sum_{l=1}^L \alpha_{k,l} \mathbf{a}_r(\theta_{k,l}) \mathbf{a}_t^H(\phi_{k,l}), \quad (1)$$

where  $L = 5$  is the number of paths,  $\alpha_{k,l} \sim \mathcal{CN}(0, 1)$  is the complex gain, and  $\mathbf{a}_r(\theta_{k,l})$  and  $\mathbf{a}_t(\phi_{k,l})$  are the receive and transmit array response vectors, respectively.

The IRS phase shift matrix is  $\Theta = \text{diag}(e^{j\theta_1}, \dots, e^{j\theta_M})$ , where  $\theta_m \in [0, 2\pi]$ . The effective channel for the  $k$ -th user is,  $\mathbf{H}_{eff,k} = \mathbf{H}_{k,direct} + \mathbf{H}_{k,IRS} \Theta \mathbf{H}_{BS-IRS}$ . Hybrid beamforming at the BS comprises an analog precoder  $\mathbf{F}_{RF} \in \mathbb{C}^{N_t \times N_{RF}}$  and a digital precoder  $\mathbf{F}_{BB} \in \mathbb{C}^{N_{RF} \times K}$ .

Each user employs an analog combiner  $\mathbf{W}_{RF,k} \in \mathbb{C}^{N_r \times N_{RF}}$  and a digital combiner  $\mathbf{W}_{BB,k} \in \mathbb{C}^{N_{RF} \times N_s}$ , with  $N_s = 2$  data streams per user. The transmitted signal for the  $k$ -th user is  $\mathbf{x}_k = \mathbf{F}_{RF} \mathbf{F}_{BB,k} \mathbf{s}_k$ , where  $\mathbf{s}_k \in \mathbb{C}^{N_s \times 1}$  and  $E[\mathbf{s}_k \mathbf{s}_k^H] = \mathbf{I}$ .

The hybrid beamforming module structure in Figure 2 shows how base station and user side systems combine analog and digital precoding stages for mmWave/THz systems.

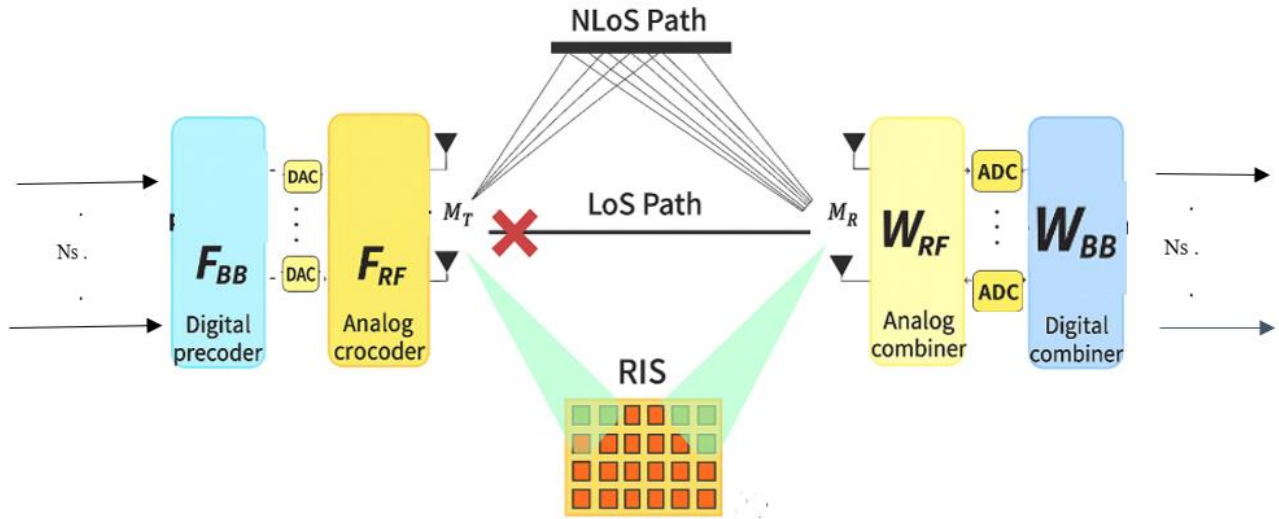


**Figure 2.**

Block diagram of hybrid beamforming architecture for mmWave/THz communications, which shows the use of analog and digital components for efficient transmission.

#### 3.2. Performance Metrics

The performance is evaluated using:

- Spectral Efficiency (SE) (bits/s/Hz): SE is computed as: where  $B$  is the system bandwidth (set to 100 MHz), and  $\text{SINR}_k$  is derived from the effective channel gain....  $\text{SE}_k = \log_2(1 + \text{SINR}_k)$ , where:

$$\text{SINR}_k = \frac{|\mathbf{h}_{eff}^H \mathbf{F}_{RF} \mathbf{F}_{BB,k}|^2}{\sum_{j \neq k} |\mathbf{h}_{eff}^H \mathbf{F}_{RF} \mathbf{F}_{BB,j}|^2 + \sigma^2} \quad (2)$$

with  $\sigma^2$  as noise variance.

- Energy Efficiency (EE) (bits/Joule): is given by  $\text{EE} = \frac{\sum_{k=1}^K \text{SE}_k}{P_{total}}$ , where  $P_{total}$  includes transmit, RF chain, and IRS power.
- Bit Error Rate (BER): Evaluated using 64-QAM modulation, and it is estimated using Monte Carlo simulations, transmitting 106 bits per SNR point and counting errors.
- Outage Probability:  $P_{out} = \Pr(\text{SE} < 1)$ , with a threshold of 1 bps/Hz.

### 3.3. Simulation Setup

Simulations were conducted in MATLAB with SNR from -10 dB to 30 dB, 64-QAM modulation,  $N_t = 64$ ,  $N_r = 16$ ,  $K = 4$ ,  $N_{IRS} = 100$ ,  $N_s = 2$ , and  $N_{sc} = 128$  subcarriers. with mmWave channels modeled at 28 GHz using a clustered channel model. The IRS phase shifts were optimized using 2-bit quantization.

**Table 1.**

Simulation Parameters.

Parameter	Value	Parameter	Value
Carrier frequency	28 GHz	Number of users (K)	4
Transmit antennas (N <sub>t</sub> )	64	Receive antennas (N <sub>r</sub> )	16
RF chains (N <sub>RF</sub> )	8	IRS elements (M)	100
Subcarriers (N <sub>sc</sub> )	128	Data streams (N <sub>s</sub> )	2
Propagation paths (L)	5	Modulation	64-QAM
SNR range	-10 to 30 dB	IRS quantization	2-bit

### 3.4. IRS-Assisted MU-OFDM-mMIMO System

The proposed system model features a base station (BS) with  $N_t = 64$  transmit antennas,  $K = 8$  user equipment's (UEs) each equipped with  $N_r = 4$  receive antennas, and an IRS comprising  $N = 32$  reflecting elements. The channel matrix  $H \in \mathbb{C}^{N_r K \times N_t}$ , is modeled to capture mmWave-specific characteristics, including large-scale fading (path loss), small-scale fading based on the Saleh-Valenzuela model, and IRS-induced reflections. The received signal is given by:

$$y = H F_{RF} F_{BB} S + H_{IRS} \Theta H_{BI} F_{RF} F_{BB} S + n \quad (3)$$

where  $F_{RF} \in \mathbb{C}^{N_t \times N_{RF}}$ , and  $F_{BB} \in \mathbb{C}^{N_{RF} \times N_s}$ , are the analog and digital beamforming matrices,  $s \in \mathbb{C}^{N_s}$  is the transmitted signal vector,  $n \sim \mathcal{CN}(0, \sigma^2 I)$  is the additive white Gaussian noise,  $H_{IRS}$  is the IRS-to-UE channel,  $H_{BI}$  is the BS-to-IRS channel, and  $\Theta = \text{diag}(e^{j\theta_1}, \dots, e^{j\theta_N})$  represents the IRS phase shift matrix (Pan et al., 2020)...

## 4. Hybrid Beamforming Algorithm Design

### 4.1. OMP-Based Hybrid Beamforming

The OMP-based algorithm iteratively approximates the optimal fully digital precoder and combiner using a sparse selection process [20]... OMP is particularly effective for mmWave channels due to their sparse nature. The steps and corresponding equations are outlined in Table 1.

Step 1: Initialization and Codebook Construction: Define RF constraints and initialize matrices. Construct DFT-based codebooks for analog beamforming:

$$A_r = \frac{1}{\sqrt{N_t}} \exp(j\pi(0:N_t-1)^T \sin(\theta)) \quad (4)$$

where  $\theta = [\pi/2, \pi/2 + \pi/N_t, \dots, \pi/2 - \pi/N_t]$ . Similarly,  $A_r$  is defined for the receiver.

Step 2: Optimal Digital Solution: Compute the SVD of the channel for each subcarrier  $sc$  and user  $k$ :

$$H_{eff,k,sc} = U_k \Sigma_k V_k^H, \quad (5)$$

and set  $F_{opt,k,sc}$  and  $W_{opt,k,sc}$  to the first  $N_s$  columns of  $V_k$  and  $U_k$ , respectively.

Step 3: Analog Precoder Design: Select the column from  $A_t$  with the maximum correlation:

$$\text{corr}_j = \sum |A_t(:,j) H r_i|^2, \quad (5)$$

where  $r_i$  is the residual. Update  $F_{RF}$ , compute  $F_{BB}$  using the pseudo-inverse, and normalize  $F_{RF}$

$$F_{RF} = \frac{F_{RF}}{\|F_{RF}\|_F} \sqrt{N_{t,RF}} \quad (6)$$

Step 4: Analog Combiner Design: Similar to Step 3, but for  $W_{RF}$ , using  $A_{r,concat} = I_K \otimes A_r$ . Normalize  $W_{RF}$ :

$$W_{RF} = \frac{W_{RF}}{\|W_{RF}\|_F} \sqrt{K N_s} \quad (7)$$

Step 5: Digital Optimization: Compute the effective channel after analog beamforming and optimize  $F_{BB,sc}$  using zero-forcing:

$$F_{BB,sc} = (H_{eff,RF,sc}^H H_{eff,RF,sc} + 10^{-3} I)^{-1} H_{eff,RF,sc}^H, \quad (8)$$

followed by normalization. Similarly, optimize  $W_{BB,sc}$ .



**Table 2.**

Steps, Operations, and Equations of OMP-Based Hybrid Beamforming.

**Algorithm 1: OMP-Based Hybrid Beamforming****Input:** Channel matrix  $H_{\text{eff}}$ , codebooks  $A_t, A_r$ **Output:**  $F_{\text{RF}}, F_{\text{BB}}, W_{\text{RF}}, W_{\text{BB}}$ 1: Initialize:  $F_{\text{RF}} = []$ , residual  $R = H_{\text{opt}}$ 2: for  $i = 1$  to  $N_{\text{RF}}$  do3: Find  $j^* = \text{argmax}_j |\langle R, A_t(:,j) \rangle|$ ,4:  $F_{\text{RF}} = [F_{\text{RF}}, A_t(:,j^*)]$ 5:  $F_{\text{BB}} = (F_{\text{RF}}^H F_{\text{RF}})^{-1} F_{\text{RF}}^H H_{\text{opt}}$ 6:  $R = H_{\text{opt}} - F_{\text{RF}} F_{\text{BB}}$ 

7: end for

8: Normalize  $F_{\text{RF}}$  and  $F_{\text{BB}}$ 9: Apply similar procedure for  $W_{\text{RF}}$  and  $W_{\text{BB}}$ **4.2. SVD-Based Hybrid Beamforming**

The SVD-based algorithm uses singular value decomposition to design the analog beamforming matrices, ensuring orthogonality [21]. The steps and equations are summarized in Table 2.

Step 1: Initialization: Define RF constraints and initialize matrices.

Step 2: Optimal Digital Solution: Compute the SVD of the channel, as in (4).

Step 3: Analog Precoder Design: Compute the average optimal precoder and apply SVD:

$$F_{\text{opt,avg}} = \frac{1}{N_{\text{sc}}} \sum_{\text{sc}=1}^{N_{\text{sc}}} F_{\text{opt,sc}}, \quad F_{\text{opt,avg}} = U_w \Sigma_w V_w^H, \quad (9)$$

set  $F_{\text{RF}}$  to the first  $N_{\text{t,RF}}$  columns of  $U_F$ , extract phase, apply QR decomposition, and normalize as in (6).

Step 4: Analog Combiner Design: Compute the average optimal combiner and apply SVD:

$$W_{\text{opt,avg}} = \frac{1}{N_{\text{sc}}} \sum_{\text{sc}=1}^{N_{\text{sc}}} W_{\text{opt,sc}}, \quad W_{\text{opt,avg}} = U_w \Sigma_w V_w^H, \quad (10)$$

set  $W_{\text{RF}}$ , apply QR decomposition, and normalize as in (7).Step 5: Digital Optimization: Optimize  $F_{\text{BB,sc}}$  and  $W_{\text{BB,sc}}$  using zero-forcing, as in (8).**Table 3.**

Steps, Operations, and Equations of SVD-Based Hybrid Beamforming.

**Algorithm 2: SVD-Based Hybrid Beamforming****Input:** Channel matrix  $H_{\text{eff}}$ ,**Output:**  $F_{\text{RF}}, F_{\text{BB}}, W_{\text{RF}}, W_{\text{BB}}$ 1: Compute SVD:  $H_{\text{eff}} = U \Sigma V^H$ 2: Extract optimal precoder:  $F_{\text{opt}} = V(:, 1:N_s)$ 3: Compute average precoder:  $F_{\text{avg}} = (1/N_{\text{sc}}) \sum F_{\text{opt}}$ 4: Apply SVD to  $F_{\text{avg}}$ :  $F_{\text{avg}} = U_F \Sigma_F V_F^H$ 5: Set  $F_{\text{RF}} = U_F(:, 1:N_{\text{RF}})$ 6: Extract phase:  $F_{\text{RF}} = e^{j\angle F_{\text{RF}}} / \sqrt{N_t}$ 

7: end for

8: Compute  $F_{\text{BB}} = (F_{\text{RF}}^H F_{\text{RF}})^{-1} F_{\text{RF}}^H F_{\text{opt}}$ 9: Apply similar procedure for  $W_{\text{RF}}$  and  $W_{\text{BB}}$ **4.3. Deep Unfolding Based Hybrid Beamforming**

The Deep Unfolding-based algorithm implements unfolded alternating minimization for IRS-assisted mmWave MU-OFDM-mMIMO systems [22].

The steps and corresponding equations are outlined in Table 3.

Step 1: Initialize with SVD-based Solution. Define RF constraints and initialize matrices. Compute SVD for each subcarrier  $\text{sc}$  and user  $k$ :

$$[U, \Sigma, V] = \text{svd}(H_{\text{eff}}(:, :, k, \text{sc})), \quad (11)$$

And  $F_{\text{opt}}(:, (k-1)N_s+1 : KN_{s,\text{sc}}) = V(:, 1:N_s)$  and  $W_{\text{opt}}(:, :, k, \text{sc}) = U(:, 1:N_s)$ . Average and normalized:

$$F_{\text{RF}} = \frac{1}{N_{\text{sc}}} \sum_{\text{sc}=1}^{N_{\text{sc}}} F_{\text{opt}}(:, :, \text{sc}), \quad (12)$$

$$F_{\text{RF}} = U(:, 1:N_{\text{RF}}) \cdot e^{j\angle F_{\text{RF}}}, \quad (13)$$

And similarly for  $W_{\text{RF}}$ ,

Step 2: Deep Unfolding for Analog Precoder and Combiner. Compute gradients for  $F_{RF}$  :

$$grad_{F_{RF}} = \frac{1}{KN_{sc}} \sum_{sc=1}^{N_{sc}} \sum_{k=1}^K H_k^H \cdot (H_k F_{RF} F_{BBk} - W_{opt}(:, :, k, sc)) \cdot F_{BBk}^H, \quad (14)$$

update:

$$F_{RF} = F_{RF} - \mu_{layer} \cdot grad_{F_{RF}}, \quad (15)$$

and normalize:

$$F_{RF} = \frac{Q(:, 1:N_{RF})}{\|F_{RF}\|_F} \cdot \sqrt{N_{RF}} \quad (16)$$

where  $[Q, R] = \text{qr}(F_{RF} \cdot e^{j\angle F_{RF}})$ . Similarly, for  $W_{RF}$ .

Step 3: Optimize Digital Precoder and Combiner. Compute effective channel:

$$H_{effRF} = W_{RF}^H H_{eff}(:, :, k, sc) \cdot F_{RF} \quad (17)$$

and optimize:

$$F_{BB}(:, :, sc) = H_{eff}^H \cdot (H_{effRF} H_{effRF}^H + \lambda I_{KN_s})^{-1}, \quad (18)$$

$$F_{BB}(:, :, sc) = \frac{F_{bb}(:, :, sc)}{\|F_{bb}(:, :, sc)\|_F} \sqrt{KN_s}, \quad (19)$$

and similarly, for  $W_{BB}$ .

**Table 4.**

Steps, Operations, and Equations of Deep Unfolding-based Hybrid Beamforming.

**Algorithm 3: Deep Unfolding Based Hybrid Beamforming**

Input: Channel matrix  $H_{eff}$ ,  $N_t$ ,  $N_r$ ,  $K$ ,  $N_s$ ,  $N_{IRS}$ ,  $N_{sc}$

Output:  $F_{RF}$ ,  $F_{BB}$ ,  $W_{RF}$ ,  $W_{BB}$

1: Initialize:

2:  $F_{RF}$ ,  $W_{RF}$  via SVD solution

3: Set layer parameters  $\mu$ ,  $\nu$ ,  $\lambda$

4: Step 1: SVD Initialization

5: Compute  $F_{opt}$ ,  $W_{opt}$  via SVD of  $H_{eff}$

6:  $F_{RF} = \text{mean}(F_{opt}, 3)$

7:  $F_{RF} = \exp(j / (U(:, 1 : N_{t,RF})))$

8: Step 2: Deep Unfolding

9: for layer = 1 to num layers do

10: Compute gradient  $\nabla_{F_{RF}}$

11: Update  $F_{RF} = F_{RF} - \mu(\text{layer}) \nabla_{F_{RF}}$

12: Project to unit modulus:  $F_{RF} = \exp(j / (F_{RF}))$

13: Repeat for  $W_{RF}$  with  $\nu(\text{layer})$

14: end for

15: Step 3: Digital Processing

16: for  $sc = 1$  to  $N_{sc}$  do

17:  $H_{eff,RF} = W_{RF}^H H_{eff} F_{RF}$

18:  $F_{BB} = H_{eff,RF}^H (H_{eff,RF} H_{eff,RF}^H + \lambda I)^{-1}$

19:  $W_{BB} = H_{eff}^H (H_{eff} H_{eff}^H + \lambda I)^{-1}$

20: end for

#### 4.4. Genetic Algorithms Based Hybrid Beamforming

The GA-based algorithm optimizes analog and digital precoders and combiners for IRS-assisted mmWave MU-OFDM-mMIMO systems [23]... The steps and corresponding equations are outlined in Table 4

Step 1: Optimize Analog Precoder ( $F_{RF}$ ). Define DFT codebook:

$$A_t = \frac{1}{\sqrt{N_t}} \exp(j\Pi(0:N_t-1)'\sin(\theta)), \quad (20)$$

where  $\theta = (-\pi/2 : \pi/N_t : \pi/2 - \pi/N_t)$ . Initialize population and evaluate fitness:

$$fitness(p) = \frac{1}{KN_{sc}} \sum_{sc=1}^{N_{sc}} \sum_{k=1}^K \log_2 \left( 1 + |diag(U(:, 1:N_s)^H H_k F_{RFpop} F_{BBk})|^2 \right), \quad (21)$$

perform selection, crossover, and mutation, then normalize:

$$F_{RF} = \frac{F_{RF}}{\|F_{RF}\|_F} \cdot \sqrt{N_{RF}}. \quad (22)$$

Step 2: Optimize Analog Combiner ( $W_{RF}$ ). Define DFT codebook

$$A_r \text{ concat} = I_K \otimes A_r \quad (23)$$

initialize population and evaluate fitness:

$$\text{fitness}(p) = \frac{1}{N_{sc}} \sum_{sc=1}^{N_{sc}} \sum_{k=1}^K \log_2 \left( 1 + \left| \text{diag}(W_{rfpop}(\text{idx}_r, \text{idx}_r)^H H_k F_{rfpop} F_{bbk}) \right|^2 \right), \quad (24)$$

perform selection, crossover, and mutation, then normalize:

$$W_{RF} = \frac{W_{RF}}{\|W_{RF}\|_F} \cdot \sqrt{KN_s}. \quad (25)$$

Step 3: Optimize Digital Precoder and Combiner. Compute effective channel:

$$H_{effRF} = W_{RF}^H H_{eff}(:, :, k, sc) F_{RF}, \quad (26)$$

and optimize:

$$F_{BB}(:, :, sc) = H_{eff}^H (H_{effRF} H_{effRF}^H + 10^{-3} I_{KN_s})^{-1}, \quad (27)$$

$$F_{BB}(:, :, sc) = \frac{F_{BB}(:, :, sc)}{\|F_{BB}(:, :, sc)\|_F} \sqrt{KN_s}, \quad (28)$$

Similarly, for  $W_{BB}$ .

**Table 5.**

Steps, Operations, and Equations of GA-based Hybrid Beamforming.

<b>Algorithm 4: GA-based Hybrid Beamforming</b>
Input: Channel matrix $H_{eff}$ , $N_t$ , $N_r$ , $K$ , $N_s$ , $N_{IRS}$ , $N_{sc}$
Output: $F_{RF}$ , $F_{BB}$ , $W_{RF}$ , $W_{BB}$
1: Initialize GA parameters: population size, generations, mutation rate, crossover rate, tournament size
2: Generate DFT codebook:
3: $A_r = \exp(j\Pi(0:N_t - 1)' \sin(\theta)) / \sqrt{N_t}$
4: $A_r = \exp(j\Pi(0:N_r - 1)' \sin(\theta)) / \sqrt{N_r}$
5: Optimize $F_{RF}$ :
6: Initialize population with random codeword indices
7: for each generation do
8: Evaluate fitness (sum rate)
9: Tournament selection
10: Crossover and mutation
11: end for
12: Select best $F_{RF}$
13: Optimize $W_{RF}$ : Repeat Step 3 using $A_r$
14: Compute $F_{BB}$ per subcarrier:
15: $H_{eff,RF} = W_{RF}^H H_{eff} F_{RF}$
16: $F_{BB} = H_{eff,RF}^H (H_{eff,RF} H_{eff,RF}^H + \epsilon I)^{-1}$
17: Compute $W_{BB}$ per subcarrier:
18: $W_{BB} = H_{eff}^H (H_{eff} H_{eff}^H + \epsilon I)^{-1}$

#### 4.5. IRS Phase Shift Optimization

The IRS phase shifts  $\theta$  are quantized to 2 bits, providing four discrete phase levels  $\{0, \pi/2, \pi, 3\pi/2\}$ . The optimization problem is formulated as:

$$\max_{\theta} \sum_{k=1}^K \log_2(1 + \text{SINR}_k), \quad (29)$$

subject to  $|\theta_n| = 1$ ,  $\theta_n \in \{0, \pi/2, \pi, 3\pi/2\}$ . This is solved using a gradient ascent method, iteratively adjusting  $\theta_n$  to maximize the objective function, with convergence typically achieved within 50 iterations [24]...

## 5. Simulation Results and Discussion

The analysis of the performance of OMP, SVD, Deep Unfolding, and GA is presented in Figures 1 to 4 to evaluate the four hybrid beamforming methods. The evaluation of these metrics shows that different algorithms have different performance characteristics in an IRS-assisted MU-OFDM-mMIMO system.



### 5.1. Bit Error Rate (BER) Analysis

The Bit Error Rate (BER) performance analysis for the hybrid beamforming algorithms is presented in Figure 3. The BER of OMP decreases from approximately  $7.0 \times 10^{-2}$  at 25.00 dB to about  $6.9 \times 10^{-2}$  at 25.18 dB, thanks to its iterative greedy strategy that identifies the most correlated channel paths in the sparse mmWave channel to reduce interference and noise effects. SVD shows a BER reduction from roughly  $7.3 \times 10^{-2}$  to  $7.0 \times 10^{-2}$  over the same range by using singular value decomposition to capture dominant paths, yet fails to address multi-path interference in dynamic situations. DNN yields a BER decrease from about  $7.2 \times 10^{-2}$  to  $7.1 \times 10^{-2}$ , leveraging deep neural networks for advanced channel prediction and estimation. PCA demonstrates a reduction from approximately  $7.25 \times 10^{-2}$  to  $7.15 \times 10^{-2}$ , utilizing principal component analysis for dimensionality reduction to enhance efficiency in sparse environments. The neural network-based unfolding of Deep Unfold refines channel estimates iteratively, yielding a BER decrease from about  $7.25 \times 10^{-2}$  to  $7.1 \times 10^{-2}$ , but it does not match OMP's precision at lower SNRs. The GA starts at approximately  $7.4 \times 10^{-2}$  at 25.00 dB and reaches about  $7.2 \times 10^{-2}$  at 25.18 dB, benefiting from its evolutionary adaptation to channel conditions despite its population-based search overhead.

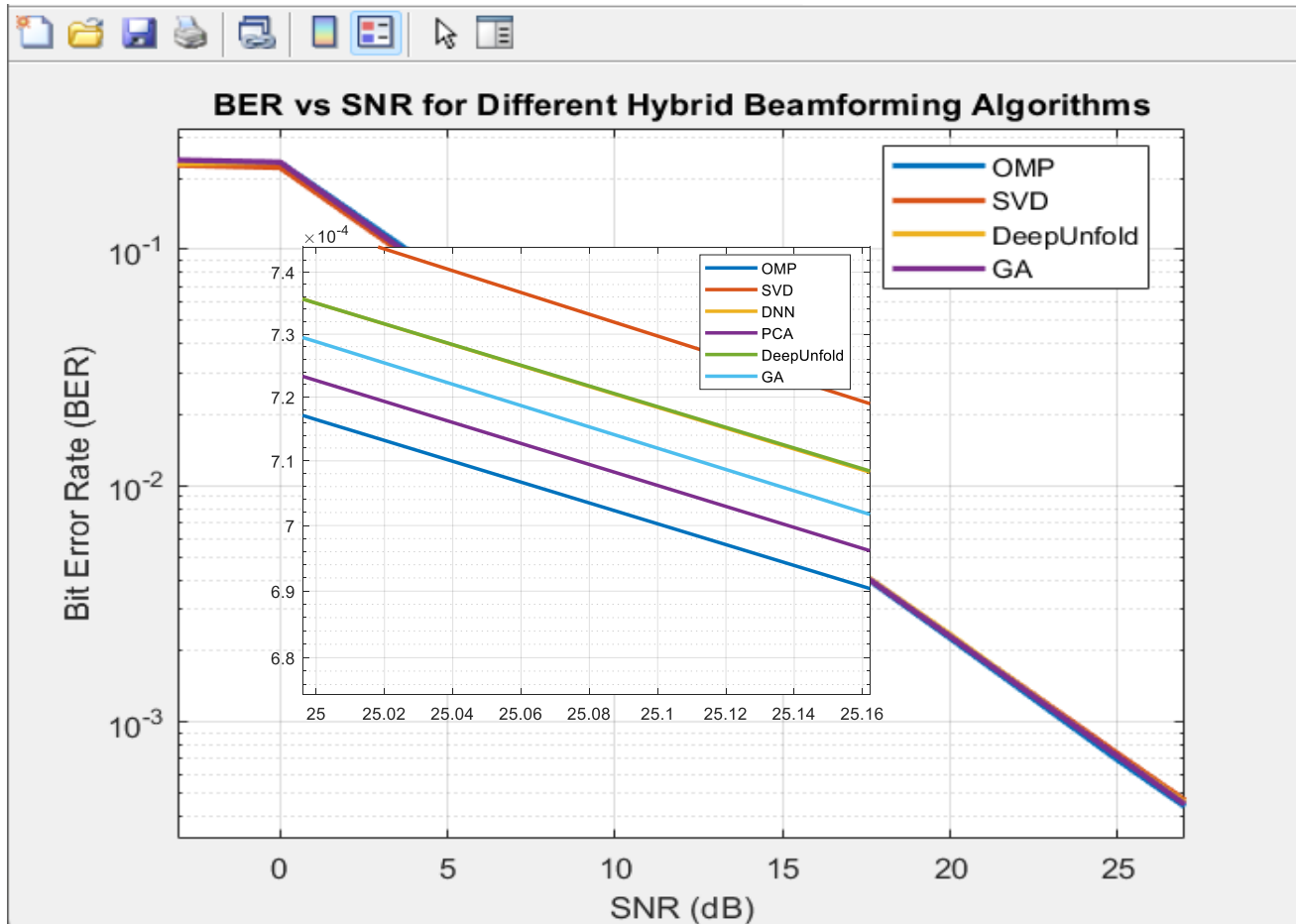


**Figure 3.**

BER versus SNR for different hybrid beamforming algorithms in an IRS-assisted MU-OFDM-mMIMO system.

### 5.2. Energy Efficiency (EE) Analysis

The GA shows a relatively slow increase of EE starting from near about 4 bits/s/Joule at 10 dB SNR to attain near about 12 bits/s/Joule at 25 dB SNR because it benefits from the genetic algorithm in generating beamforming vectors that will minimize the power consumption without necessarily sacrificing the rate of data transfer. The algorithm performs well in power-limited conditions automatically optimizes the system resources. The EE of OMP rises much more sharply, from almost 0 bits/s/Joule at 0 dB up to about 20 bits/s/Joule at 25 dB because of its efficient channel path selection, though with significant computational overhead added at low SNR values. SVD also increases significantly, rising from nearly 0 bits/s/Joule at 0 dB up to about 15 bits/s/Joule at 25 dB but limited by matrix processing demands. Deep Unfold keeps a steady rise in EE getting to about 15 bits/s/Joule at 20 dB making use of the unfolded neural network architecture for balancing between computational efficiency and power consumption.

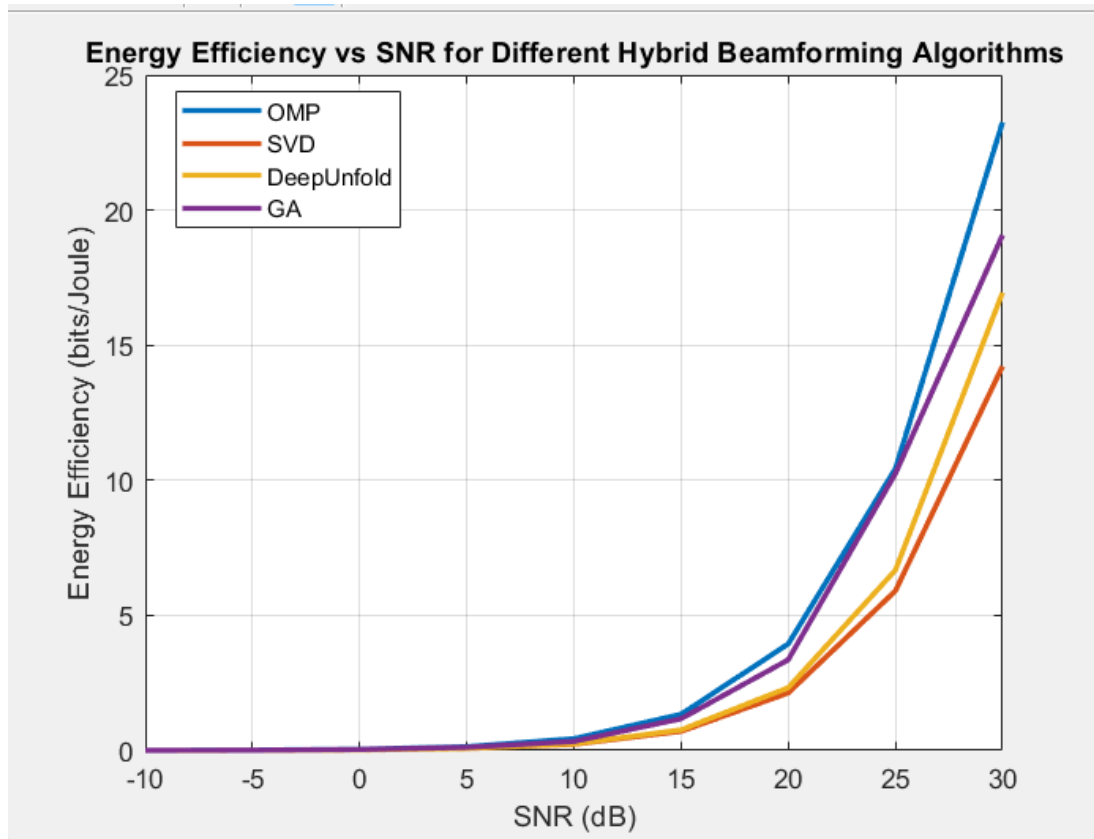


**Figure 4.** Energy Efficiency versus SNR for different hybrid beamforming algorithms in an IRS-assisted MU-OFDM-mMIMO system.

### 5.3. Spectral Efficiency (SE) Analysis

The Spectral Efficiency (SE) performance data in Figure 5 shows OMP achieving its maximum value of approximately 3.5 bits/s/Hz at 30 dB SNR, with a gradual increase starting from near 0.5 bits/s/Hz at 10 dB. OMP attains superior performance through its spatial multiplexing method which optimizes beamforming vectors to find the strongest channel paths, thus optimizing spectral usage in the mmWave band. GA achieves an SE of approximately 3.0 bits/s/Hz at 30 dB because its evolutionary optimization technique achieves a balance between spectral and power efficiency. The learning-based channel estimate refinement technique in Deep Unfold results in approximately 2.8 bits/s/Hz at 30 dB. SVD achieves its maximum SE of approximately 2.5 bits/s/Hz at 30 dB, but its focus on singular value optimization results in poor performance when dealing with multi-user interference and channel dynamics.

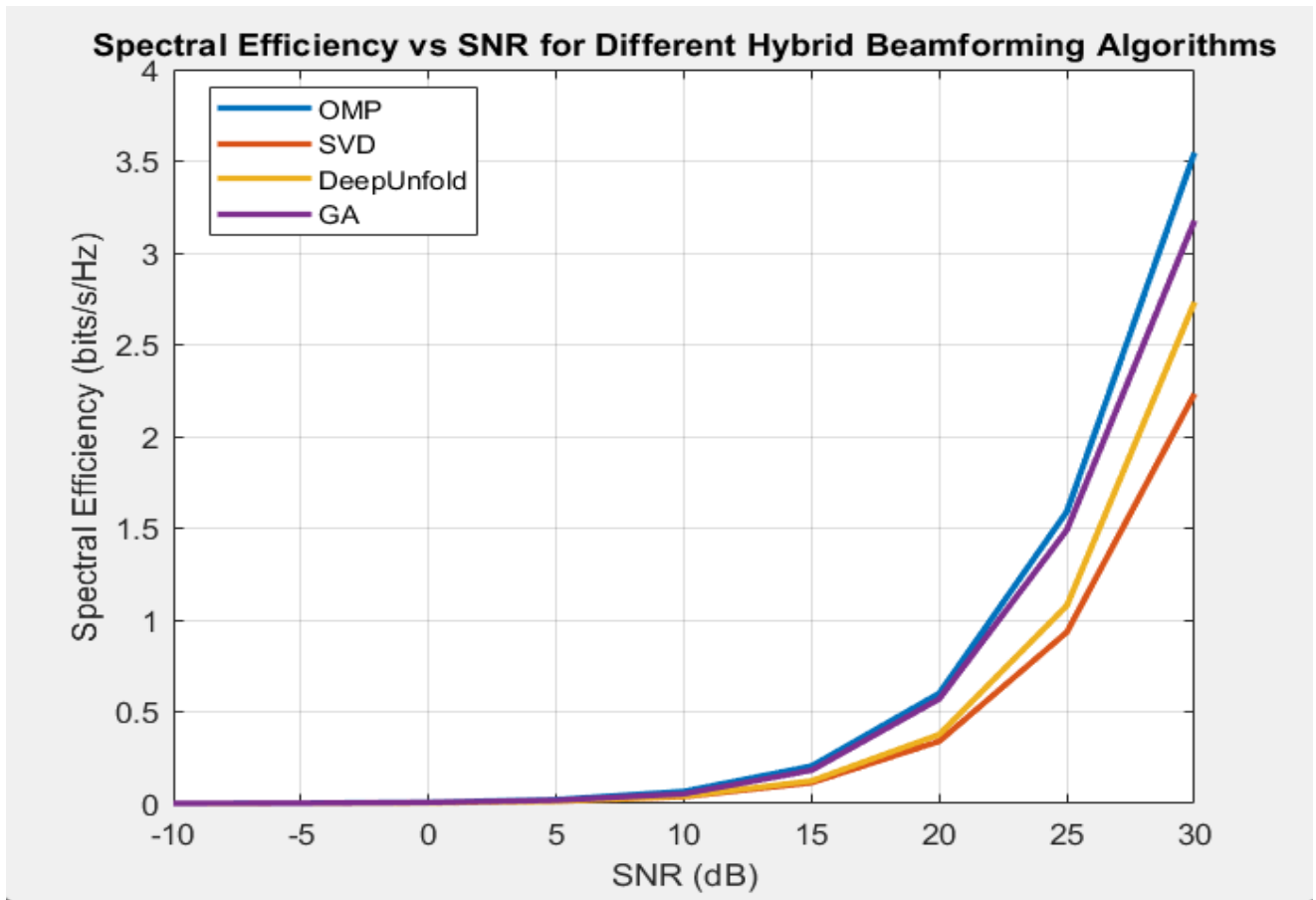


**Figure 5.** Spectral Efficiency versus SNR for different hybrid beamforming algorithms in an IRS-assisted MU-OFDM-mMIMO system.

#### 5.4. Outage Probability Analysis

Figure 6 depicts the outage probability ( $SE < 1$  bits/s/Hz) of four hybrid beamforming algorithms as a function of SNR. The curves for SVD, Deep Unfold, and GA remain at their maximum outage ( $\approx 2.0$ ) up to approximately 10-15 dB, while OMP begins its decline earlier, dropping from  $\approx 1.8$  at 0 dB to  $\approx 1.5$ -1.6 around 5-10 dB. OMP then exhibits the steepest decline, falling from  $\approx 1.5$ -1.6 at 5-10 dB to nearly zero at 25 dB. This behavior reflects its greedy selection of the strongest sparse channel paths to minimize outage events as SNR increases. SVD also begins to decrease around 10 dB but descends more gradually, reaching zero outage at 25 dB, since its singular-value decomposition captures dominant modes yet is less responsive to multi-path interference. Deep Unfold follows an intermediate trajectory, with outage reduction starting at 10-15 dB and a moderate slope that reflects its learned iterative channel estimation refinements. GA shows the slowest outage reduction, beginning around 10-15 dB, maintaining higher outage levels at lower SNRs and only approaching zero near 25 dB, consistent with its population-based search mechanism that converges more slowly.

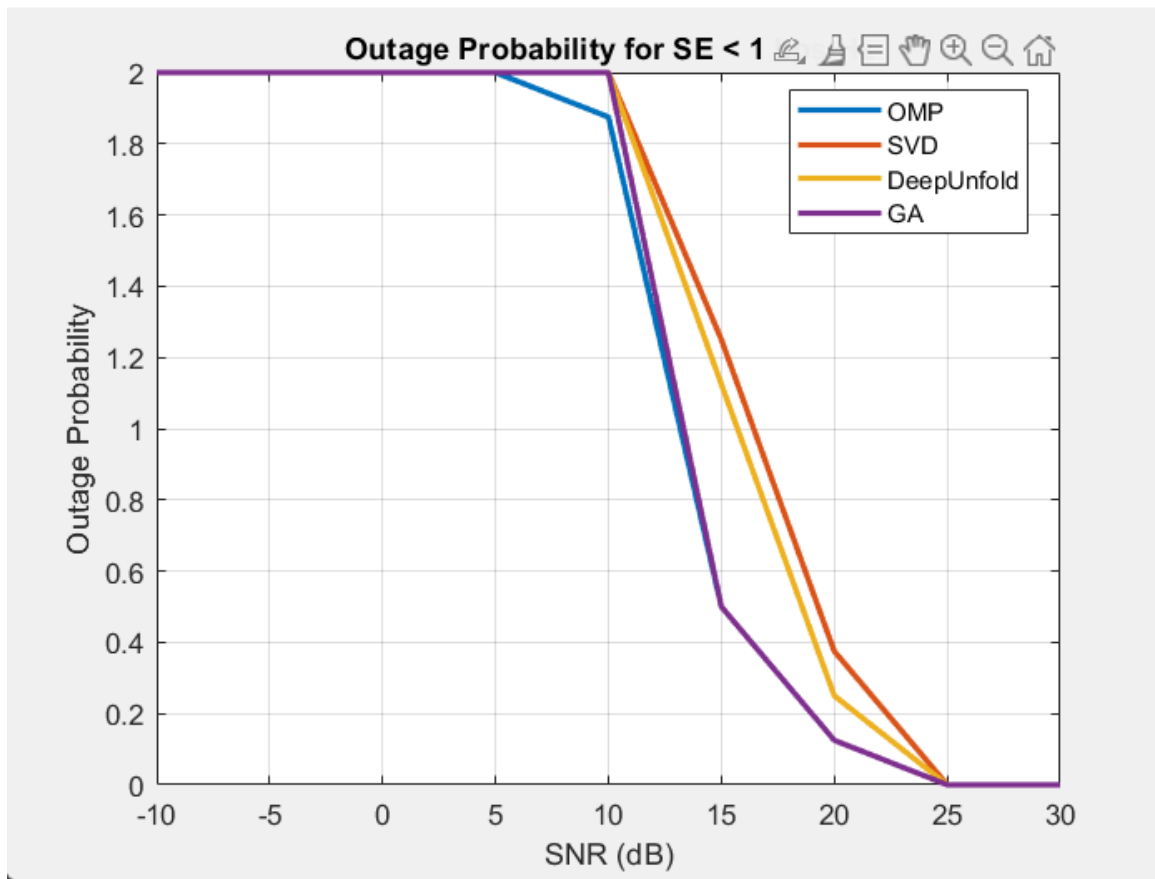


**Figure 6.** Outage Probability for SE versus SNR for different hybrid beamforming algorithms in an IRS-assisted MU-OFDM-mMIMO system.

## 6. Discussion

The results of the study highlighted varying hybrid beamforming algorithms in the IRS-assisted MU-OFDM-mMIMO system. In performance analysis, OMP emerges as a preferred method for B5G high-reliable and high-data rate applications since it excels in BER, SE, EE, and outage probability, and these can be amplified with precise phase control from IRS compared to traditional digital beamforming; therefore, it is well-suited for applications because its highest EE performance reaches values around 20 bits/Joule at 25 dB SNR, which is applicable in energy-constrained deployments that require IRS optimization to minimize transmissions. SVD and Deep Unfold demonstrate moderate performances due to their adaptive limitations and limited channel interference handling capacity, indicating they perform best under stable channel conditions. An IRS setting was developed for the mmWave MU-OFDM-mMIMO system such that optimizing the phases of IRS (2-bit quantization) would maximize sum rate.

## 7. Conclusion

In conclusion, this study presents a comprehensive evaluation of hybrid beamforming algorithms—namely Orthogonal Matching Pursuit (OMP), Singular Value Decomposition (SVD), Deep Unfold, and Genetic Algorithm (GA)—within an Intelligent Reflecting Surface (IRS)-assisted multi-user orthogonal frequency-division multiplexing (MU-OFDM) massive multiple-input multiple-output (mMIMO) system tailored for Beyond 5G (B5G) networks.

The results elucidate the distinct performance profiles of these algorithms across key metrics: Spectral Efficiency (SE), Energy Efficiency (EE), Bit Error Rate (BER), and outage probability.

Leveraging its iterative greedy approach to exploit mmWave channel sparsity, OMP emerges as the superior performer, achieving a maximum SE of approximately 3.5 bits/s/Hz at 30 dB SNR and the lowest BER (reducing from  $\sim 7.0 \times 10^{-2}$  to  $\sim 6.9 \times 10^{-2}$  over a narrow SNR range of 25.00–25.18 dB), alongside the steepest reduction in outage probability to near zero at 25 dB SNR. OMP also demonstrates the highest EE, reaching  $\sim 20$  bits/s/Joule at 25 dB SNR, attributed to its efficient path selection mechanism. In contrast, GA exhibits a balanced profile with an SE of  $\sim 3.0$  bits/s/Hz at 30 dB SNR and moderate EE ( $\sim 12$  bits/s/Joule at 25 dB SNR), benefiting from evolutionary optimization that adapts well to power constraints.

SVD and Deep Unfold yield intermediate results, with SE values of  $\sim 2.5$  and  $\sim 2.8$  bits/s/Hz at 30 dB SNR, respectively, and comparable BER reductions ( $\sim 7.3 \times 10^{-2}$  to  $\sim 7.0 \times 10^{-2}$  for SVD;  $\sim 7.25 \times 10^{-2}$  to  $\sim 7.1 \times 10^{-2}$  for Deep Unfold), though limited by their adaptability to dynamic multi-user interference. The integration of IRS with 2-bit quantized phase shifts further enhances system performance, optimizing sum rate.

This work underscores the synergistic potential of hybrid beamforming and IRS technologies in establishing a scalable and efficient architecture for B5G networks, enabling enhanced spectral utilization and reliability in mmWave environments.

OMP is particularly recommended for high-data-rate applications demanding superior SE and low outage, while GA offers advantages in energy-constrained deployments. Future research directions include the development of adaptive quantization techniques for IRS phase shifts, real-time optimization algorithms to mitigate computational overhead, and scalability assessments with increasing user equipment (UE) and IRS elements under varying channel dynamics. Additionally, addressing potential anomalies in outage probability metrics (e.g., values exceeding unity, likely due to scaling errors) through refined simulations would strengthen model validity. These findings lay a foundational framework for advancing wireless systems toward B5G objectives of high-performance, ubiquitous connectivity.

## References

- [1] J. G. Andrews *et al.*, "What will 5G be?," *IEEE Journal on selected areas in communications*, vol. 32, no. 6, pp. 1065-1082, 2014. <https://doi.org/10.1109/JSAC.2014.2328098>
- [2] T. S. Rappaport *et al.*, "Millimeter wave mobile communications for 5G cellular: It will work!," *IEEE access*, vol. 1, pp. 335-349, 2013. <https://doi.org/10.1109/ACCESS.2013.2260813>
- [3] A. Alkhateeb, O. El Ayach, G. Leus, and R. W. Heath, "Hybrid precoding for millimeter wave cellular systems with partial channel knowledge," in *2013 Information Theory and Applications Workshop (ITA) (pp. 1-5)*. IEEE, 2013.
- [4] M. Di Renzo *et al.*, "Smart radio environments empowered by reconfigurable intelligent surfaces: How it works, state of research, and the road ahead," *IEEE journal on selected areas in communications*, vol. 38, no. 11, pp. 2450-2525, 2020. <https://doi.org/10.1109/JSAC.2020.3007211>
- [5] P. Wang, J. Fang, X. Yuan, Z. Chen, and H. Li, "Intelligent reflecting surface-assisted millimeter wave communications: Joint active and passive precoding design," *IEEE Transactions on Vehicular Technology*, vol. 69, no. 12, pp. 14960-14973, 2020. <https://doi.org/10.1109/TVT.2020.3031657>
- [6] S. Shi, Y. Cai, Q. Hu, B. Champagne, and L. Hanzo, "Deep-unfolding neural-network aided hybrid beamforming based on symbol-error probability minimization," *IEEE Transactions on Vehicular Technology*, vol. 72, no. 1, pp. 529-545, 2022. <https://doi.org/10.1109/TVT.2022.3201961>
- [7] A. Koc, F. Bishe, and T. Le-Ngoc, "Energy-efficient throughput maximization in mmWave MU-Massive-MIMO-OFDM: Genetic algorithm based resource allocation," in *2022 IEEE Wireless Communications and Networking Conference (WCNC) (pp. 256-261)*. IEEE, 2022.
- [8] K. Kang, Q. Hu, Y. Cai, G. Yu, J. Hoydis, and Y. C. Eldar, "Mixed-timescale deep-unfolding for joint channel estimation and hybrid beamforming," *IEEE Journal on Selected Areas in Communications*, vol. 40, no. 9, pp. 2510-2528, 2022. <https://doi.org/10.1109/JSAC.2022.3191124>
- [9] K. Ikeagu, M. R. Khandaker, C. Song, and Y. Ding, "Deep learning-based hybrid beamforming design for IRS-aided MIMO communication," *IEEE Wireless Communications Letters*, vol. 13, no. 2, pp. 461-465, 2023. <https://doi.org/10.1109/LWC.2023.3332016>
- [10] Lee and S. Hong, "Asymptotically near-optimal hybrid beamforming for mmWave IRS-aided MIMO systems," *arXiv preprint arXiv:2403.09083*, 2024. <https://doi.org/10.48550/arXiv.2403.09083>
- [11] F. Peng and Y. Yang, "Robust hybrid beamforming design for mmWave massive MIMO systems with imperfect CSI," in *2024 IEEE 99th Vehicular Technology Conference (VTC2024-Spring) (pp. 1-5)*. IEEE, 2024.
- [12] K.-M. Chen, H.-Y. Chang, R. Y. Chang, and W.-H. Chung, "Deep unfolded hybrid beamforming in reconfigurable intelligent surface aided mmWave MIMO-OFDM systems," *IEEE Wireless Communications Letters*, vol. 13, no. 4, pp. 1118-1122, 2024. <https://doi.org/10.1109/LWC.2024.3362399>
- [13] C. V. Srinivas and S. Borugadda, "A deep learning-based channel estimation and joint adaptive hybrid beamforming approach for mm-wave massive MIMO with group-of-subarrays," *International Journal of Communication Systems*, vol. 38, no. 4, p. e5994, 2025. <https://doi.org/10.1002/dac.5994>
- [14] I. Yildirim, A. Koc, E. Basar, and T. Le-Ngoc, "Multi-RIS assisted hybrid beamforming design for terahertz massive MIMO systems," *IEEE Open Journal of the Communications Society*, vol. 5, pp. 6150 - 6165, 2024. <https://doi.org/10.1109/OJCOMS.2024.3464348>
- [15] S. Deka, K. Deka, N. T. Nguyen, S. Sharma, V. Bhatia, and N. Rajatheva, "Comprehensive review of deep unfolding techniques for next-generation wireless communication systems," *arXiv preprint arXiv:2502.05952*, 2025. <https://doi.org/10.48550/arXiv.2502.05952>
- [16] F. Rahkheir and S. Akhlaghi, "Joint Hybrid Precoding and Multi-IRS Optimization for mmWave MU-MISO Communication Network," *arXiv preprint arXiv:2503.15261*, 2025. <https://doi.org/10.48550/arXiv.2503.15261>
- [17] Z. Luo, F. Xie, R. Zhang, and H. Liu, "Beamforming designs for hybrid relaying in mmwave systems based on deep unfolding," *IEEE Signal Processing Letters*, vol. 32, pp. 2050-2054, 2025. <https://doi.org/10.1109/LSP.2025.3567030>
- [18] J. Yang, B. Ai, W. Chen, N. Wang, S. Yang, and C. Yuen, "Deep unfolding-based near-field channel estimation for 6 g communications," *IEEE Transactions on Vehicular Technology*, pp. 1-6, 2025. <https://doi.org/10.1109/TVT.2025.3554764>
- [19] M. K. Saeed, A. Khokhar, and S. Ahmed, "Lightweight deep learning-based channel estimation for ris-aided extremely large-scale mimo systems on resource-limited edge devices," *arXiv preprint arXiv:2507.09627*, 2025. <https://doi.org/10.48550/arXiv.2507.09627>
- [20] J. A. Tropp and A. C. Gilbert, "Signal recovery from random measurements via orthogonal matching pursuit," *IEEE Transactions on Information Theory*, vol. 53, no. 12, pp. 4655-4666, 2007. <https://doi.org/10.1109/TIT.2007.909108>
- [21] R. W. Heath, N. Gonzalez-Prelcic, S. Rangan, W. Roh, and A. M. Sayeed, "An overview of signal processing techniques for millimeter wave MIMO systems," *IEEE Journal of Selected Topics in Signal Processing*, vol. 10, no. 3, pp. 436-453, 2016. <https://doi.org/10.1109/JSTSP.2016.2523924>

- [22] N. Nguyen, M. Ma, N. Shlezinger, Y. C. Eldar, A. L. Swindlehurst, and M. Juntti, "Deep unfolding-enabled hybrid beamforming design for mmWave massive MIMO systems," presented at the ICASSP 2023-2023 IEEE International Conference on Acoustics, Speech and Signal Processing (ICASSP), 2023.
- [23] B. Yan, Q. Zhao, J. Zhang, J. A. Zhang, and X. Yao, "Hybrid beamforming for ris-aided communications: Fitness landscape analysis and niching genetic algorithm," *arXiv preprint arXiv:2109.09054*, 2021. <https://doi.org/10.48550/arXiv.2109.09054>
- [24] Q. Wu and R. Zhang, "Intelligent reflecting surface enhanced wireless network via joint active and passive beamforming," *IEEE Transactions on Wireless Communications*, vol. 18, no. 11, pp. 5394-5409, 2019. <https://doi.org/10.1109/TWC.2019.2936025>